Supporting Information

Sensitive determination of chromium by inductively coupled plasma mass spectrometry using chelate-enhanced nebulized film dielectric barrier discharge vapor generation

Qian He,[1,2]* Chenchen Li,[2] Xiangyu Kong,[2] Minggang Zhao,[3] Jing Zhang[4,5]*

[1] *Frontiers Science Center for Deep Ocean Multispheres and Earth System, and Key Laboratory of Marine Chemistry Theory and Technology, Ministry of Education, Ocean University of China, Qingdao 266100, China*

[2]*College of Chemistry and Chemical Engineering, Ocean University of China, Qingdao, 266100, China*

[3]*Department of Materials Science and Engineering, Ocean University of China, Qingdao, 266100, China*

[4]*Faculty of Science, University of Toyama, Toyama 930-8555, Japan*

[5]*Laboratory for Marine Ecology and Environmental Science, Qingdao National Laboratory for Marine Science and Technology, Qingdao 266237, China*

**Corresponding author email: heqian@ouc.edu.cn; jzhang@sci.u-toyama.ac.jp*

Table of Contents

Sample pretreatment process.

Optimization of experimental parameters.

Table S1 The optimized ICP-MS operating parameters.

Fig. S1 The setup of chelate-enhanced NFDBD vapor generation coupled with ICP-MS for Cr determination. (GLS: gas-liquid separator)

Fig. S2 Optimization of the isotope of Cr, RF power and helium gas flow rate for Cr determination based on the ratio of signal-to-noise (S/N) by FI-NFDBD-ICP-MS system. Each data is the average from three measurements (n = 3). Error bars are defined as ± standard deviation (SD).

Fig. S3 Effect of DDTC concentration (a), solution pH (b), input discharge voltage (c) argon flow rate (d) and chelation reaction time (e) on Cr(VI) (5 μg L^{-1}) peak area in FI-NFDBD sampling system. Each data is the average of three measurements (n=3). Error bars are defined as ± SD.

Fig. S4 The blank signal profiles of Cr(VI) by only DDTC (0.005%, v/v) using FI-NFDBD sampling system with three injections.

Sample pretreatment process

Water sample: Each environmental water sample was filtered through a 0.45 μm membrane filter after collected and then kept at 4 °C until further processing. For total Cr determination, 10% (m/v) H_2O_2 was first added to the sample solution for oxidation all Cr species to Cr(VI). Considering possible matrix effect exists in the seawater sample, the Cr(VI) standard solutions of 0, 1, 2, 3 and 4 μg L^{-1} were spiked into the seawater sample individually before chelation and finally analyzed with standard addition method. The detail chelation procedure for these water samples was as follows: 10 mL of each sample solution was transferred into a 15 mL vial and 2% (v/v) nitric acid solution was added to make the final solution pH at 4.0. Then a stir bar and 25 μL of 2% DDTC in milli-Q water were added. After that, the magnetic stirrer was turned on, and the solution was stirred for 30 min to form the chelate between Cr(VI) and DDTC. Finally, the sample solution was transferred to a 30 mL Teflon bottle and injected into the FI-NFDBD-ICP-MS system for Cr(VI) determination.

Sediment sample: The sediment sample needed some digestion steps before chelation. The digestion steps were as follows: 1) 100 mg sediment sample was dissolved with 5 mL HNO_3 in a PTFE digester at 60℃, 90℃, 120℃, 150℃ and 180℃ step by step on a hot plate for 2-4 h; 2) after cooling to room temperature, 2 mL HNO_3, 2 mL HF and 2 mL $HClO_4$ were added to the PTFE digester successively under the same heat process to step 1) for continuous digestion for 3-5 h; 3) the above step of 2) was repeated again until the sample was completely digested; 4) milli-Q water was added to the digester three times (1 mL per time) to remove HF at 130℃; 5) the sample residue was completely dissolved in 1 mL 2% HNO_3 and filtered with 0.45 μm polyethersulfone membrane; 6) finally, the sample solution was diluted 80 fold with milli-Q water before chelation. The chelation process was the same to the water sample shown above. For the pH adjustment process, ammonium hydroxide was used to adjust the sample pH to 4.0 as the digested sample solution was highly acidic.

Biological tissue sample: The biological tissue sample also needed some

digestion steps before chelation. The digestion steps were as follows: 1) 1.000 g biological tissue sample was dissolved with 5 mL HNO_3 in a PTFE digester at room temperature for 24 h and then heated at 60℃, 90℃, 120℃, 150℃ and 180℃ step by step on a hot plate for 2-3 h; 2) after cooling to room temperature, 2 mL HNO_3 and 2 mL H_2O_2 were added to the PTFE digester successively under the same heat process to step 1) for continuous digestion for 3-5 h; 3) then the temperature was cooled to 140℃ to make the sample solution nearly dryness; 4) the sample residue was completely dissolved in 1 mL 2% HNO_3 and filtered with 0.45 μm polyethersulfone membrane; 5) finally, the sample solution was diluted 80 fold with milli-Q water before chelation. The chelation process was the same to the water sample shown above. For the pH adjustment process, ammonium hydroxide was used to adjust the sample pH to 4.0 as the digested sample solution was highly acidic.

Optimization of experimental parameters

For the optimization studies, the normalized mass spectrometry peak area for Cr(VI) was used for the maximum.

Effect of DDTC concentration. The effect of DDTC concentration was first investigated to study the formation condition of Cr(VI)-DDTC chelate. Various concentrations of DDTC (0.001%-0.02%, v/v) were added into the Cr(VI) standard solution (5 μg L^{-1}) for chelation at pH 4.0 and then submitted to FI-NFDBD system individually with milli-Q water as carrier. The results in Fig. S3a showed that the peak area of Cr(VI) was strongly depended on the DDTC concentration. The peak area of the Cr(VI) was increased significantly with an increase in DDTC concentration from 0.001% to 0.005% and then began to level off when the DDTC concentration was higher than 0.005%. Therefore, a DDTC concentration of 0.005% (v/v) was chosen for the determination of Cr(VI) in later experiments.

Effect of solution pH. As reported, the chelation solution pH would obviously influence the chelation efficiency between DDTC and Cr(VI),[1] thus the effect of chelation solution pH from 2.0 to 5.5 on Cr(VI) sensitivity (5 μg L^{-1}) adjusted by 2% (v/v) nitric acid was also investigated in this work. As shown in Fig. S3b, the peak

area of the Cr(VI) was increased significantly with the solution pH increased from 2.0 to 4.0 and then decreased sharply with the solution pH varied from 4.0 to 5.5. The maximum peak area of Cr(VI) was found at solution pH of 4.0, which was consistent with the optimal chelation pH between DDTC and Cr(VI) in ETV sampling system.[1] As a result, a solution pH of 4.0 was chosen for Cr(VI) determination in later studies.

Effect of input discharge voltage. Since the discharge voltage would influence the discharge intensity and the kinetic thermal temperature in DBD plasma,[2] the effect of input discharge voltage (50-250V) on Cr(VI) sensitivity (5 μg L^{-1}) was also investigated in this DDTC-enhanced FI-NFDBD vapor generation sampling system. As shown in Fig. S3c, the peak area of Cr(VI) was increased significantly with the input discharge voltage increased from 50 to 200 V and then increased slowly with the input discharge voltage varied from 200 to 250 V. Higher discharge voltage meant higher discharge intensity and higher kinetic thermal temperature in DBD plasma, which were all beneficial to improve the sensitivity of Cr(VI). However higher voltage would bring higher safety risk to the operator, thus the input discharge voltage higher than 250 V was not studied and 250 V was finally selected for further studies.

Effect of argon flow rate. The effect of argon flow rate (0.8-1.3 L min^{-1}) on Cr(VI) sensitivity (5 μg L^{-1}) in this DDTC-enhanced FI-NFDBD vapor generation sampling system was also studied, as it would affect the nebulization efficiency and the analyte concentration in the carrier gas.[3] As shown in Fig. S3d, the peak area of Cr(VI) was increased significantly with the argon flow rate increased from 0.8 to 1.1 L min^{-1} and then decreased dramatically with the argon flow rate varied from 1.1 to 1.3 L min^{-1}. Since the maximum Cr(VI) peak area was found at the argon flow rate of 1.1 L min^{-1}, this value was chosen for the later studies.

Effect of chelation reaction time. The chelation reaction time (0 - 60 min) between DDTC and Cr(VI) was studied since it also would influence the chelation efficiency. As shown in Fig. S3e, the peak area of Cr(VI) (5 μg L^{-1}) was slowly increased with the reaction time increased from 0 to 30 min and then began to level off when the reaction time was higher than 30 min. The result indicated that 30 min was enough to reach the reaction equilibrium. Therefore, the chelation reaction time

of 30 min was chosen for later experiment.

Table S1 The optimized ICP-MS operating parameters.

Parameters	Description
RF power (W)	1600
Cool gas flow rate (L min^{-1})	14.0
Auxiliary gas flow rate (L min^{-1})	0.8
Sample flow rate (mL min^{-1})	1.0
Sampling depth (mm)	5.0
Sweeps per reading	1
Dwell time (s)	0.01
Measurement mode	KED
CCT helium flow rate (mL min^{-1})	3.25
Isotopes	^{52}Cr

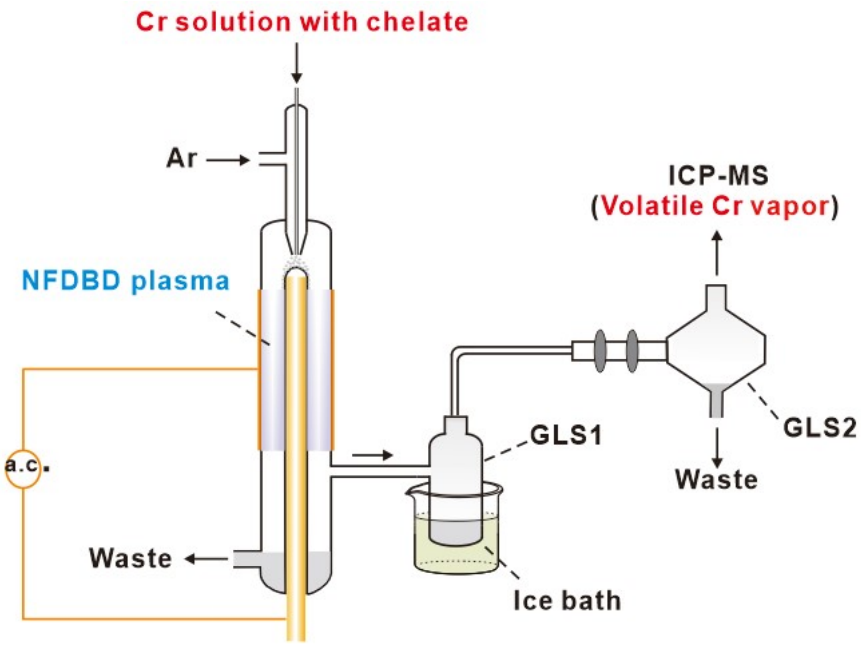

Fig. S1 The setup of chelate-enhanced NFDBD vapor generation coupled with ICP-MS for Cr determination. (GLS: gas-liquid separator)

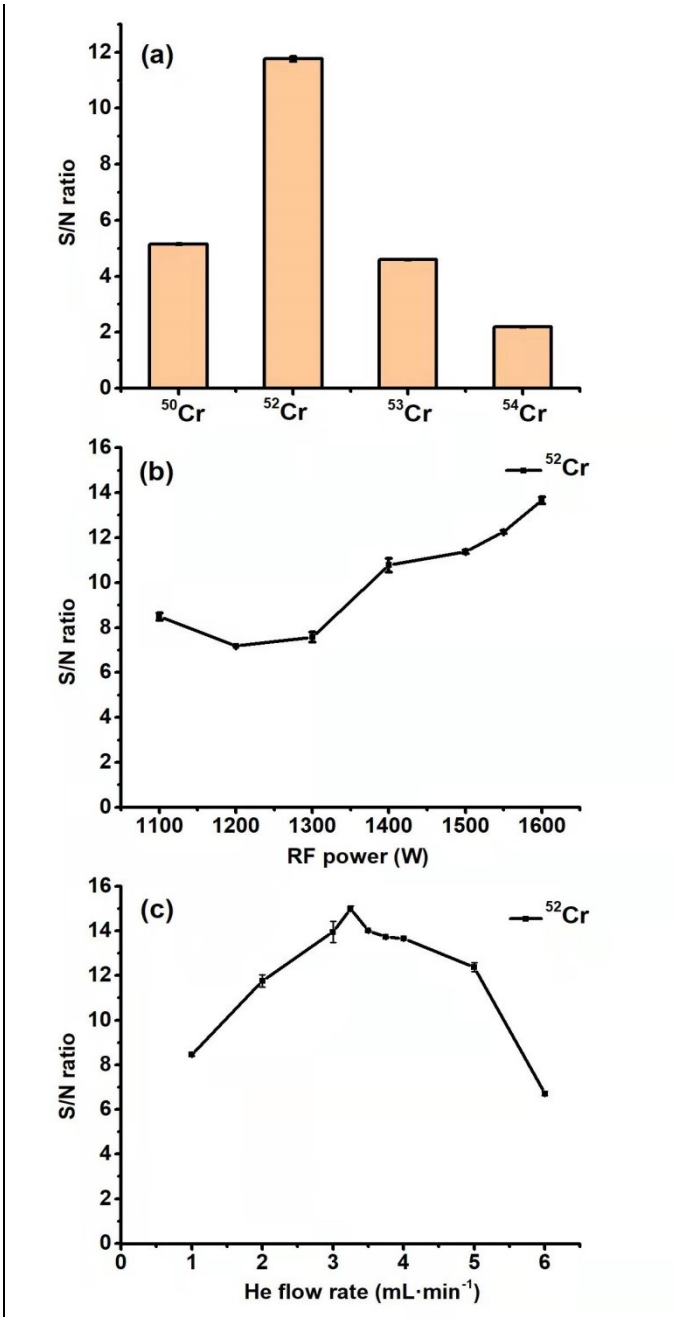

Fig. S2 Optimization of the isotope of Cr, RF power and helium gas flow rate for Cr determination based on the ratio of signal-to-noise (S/N) by FI-NFDBD-ICP-MS system. Each data is the average from three measurements (n = 3). Error bars are defined as ± standard deviation (SD).

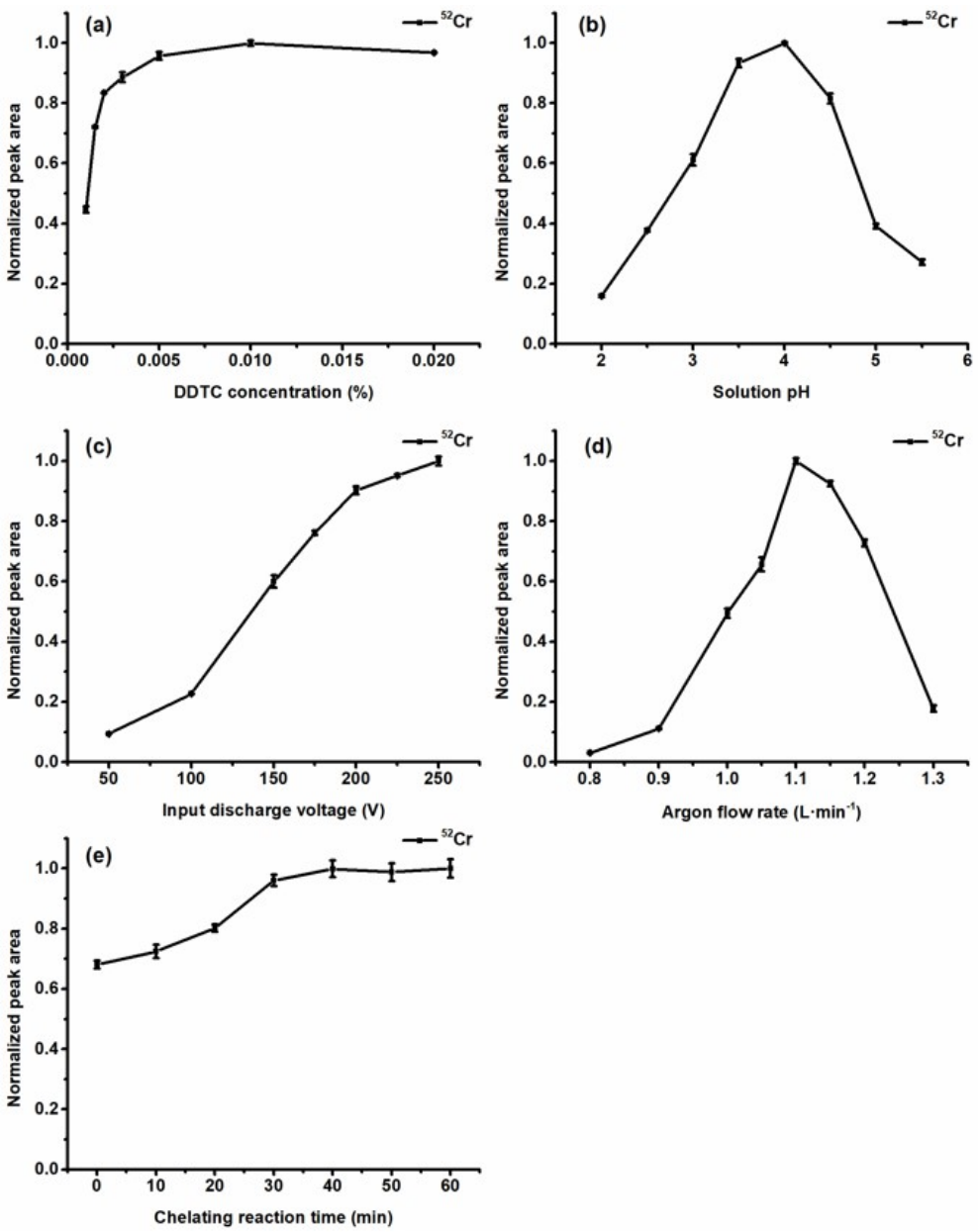

Fig. S3 Effect of DDTC concentration (a), solution pH (b), input discharge voltage (c) argon flow rate (d) and chelation reaction time (e) on Cr(VI) (5 μg L^{-1}) peak area in FI-NFDBD sampling system. Each data is the average of three measurements (n=3). Error bars are defined as ± SD.

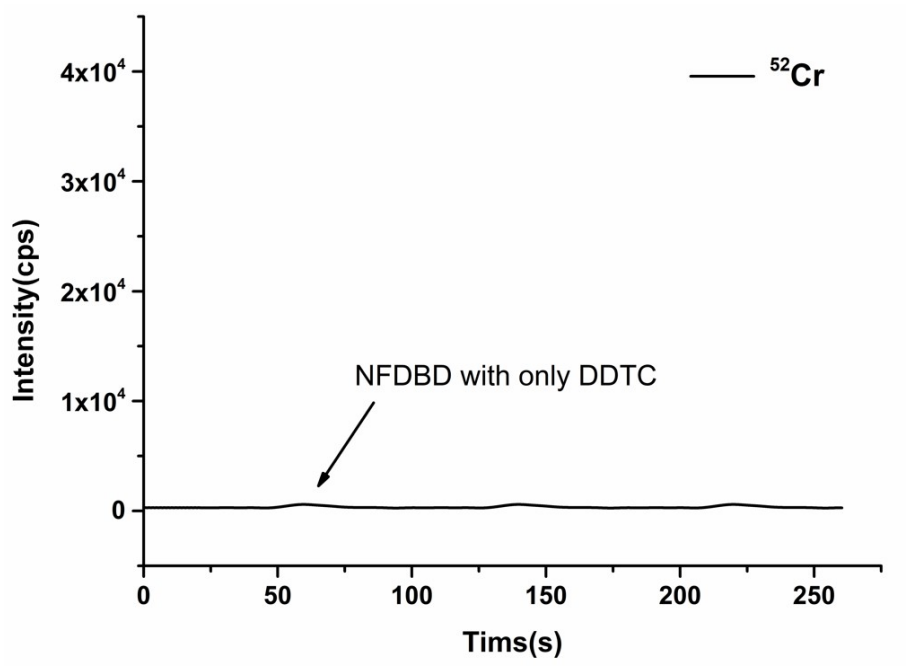

Fig. S4 The blank signal profiles of Cr(VI) by only DDTC (0.005%, v/v) using FI-NFDBD sampling system with three injections.

Reference

1 S. Chen and D. Lu, *Atom. Spectrosc*., 2012, **33**, 9-13.

2 Q. He, Y. Qiao, M. Zhao and J. Zhang, *Spectrochim. Acta Part B*, 2022, **191**, 106396.

3 Q. He, X. Wang, H. He and J. Zhang, *Anal. Chem.*, 2020, **92**, 2535-2542.